Test of local model potentials for positron scattering from rare gases

F. A. Gianturco*
Department of Chemistry, The University of Rome, 00185 Rome, Italy

Ashok Jain
Physics Department, Florida A&M University, Tallahassee, Florida 32307

J. A. Rodriguez-Ruiz
Departamento de Quimica Fisica, Universidad de Malaga, 29071 Malaga, Spain
(Received 26 April 1993; revised manuscript received 12 July 1993)

We report calculations of differential and integral cross sections for positron (e^+) scattering from He, Ne, Ar, Kr, and Xe rare gases. An optical-potential approach is employed in which the repulsive Coulombic interaction is calculated exactly at the Hartree-Fock level and the attractive polarization and correlation effects are included via a model potential determined from the use of a local density-functional theory (DFT). These model calculations are further compared with the results from two other local potentials, one based on determining the short-range correlation energy, E_C, for a positron in an homogeneous electron gas and the other from the correlation-polarization potential of an electron interacting with a free-electron gas. We found that the present DFT-based, correlation-polarization treatment is fairly simple to implement computationally and appears to be the most accurate of all the models examined here. Our results are in fact compared with recent measurements of differential and integral cross sections for positron scattering with rare gases and are found to be remarkably close to both sets of experiments.

PACS number(s): 34.80.Bm

I. INTRODUCTION

The past few years have witnessed a dramatic increase in research studies on low-energy scattering of positrons from atomic and molecular targets [1]. This increased activity is partly due to the corresponding improvements on the technology for producing reliable positron beams [2–6]. Nevertheless, there are still considerable uncertainties in the agreement between the measured values of positron-molecule cross sections at collision energies below a few eV, and away from positronium-formation thresholds [7,8], while fundamental questions about the true nature of the forces at play still plague the computations of the cross sections at such energies.

If the positronium formation and all the other inelastic channels are assumed to be small, then the full interaction between the impinging positrons and the atomic targets can be approximated as being made out of a repulsive static potential, V_{st}, and an attractive polarization potential, V_{pol}. Below the threshold for positronium formation, the most serious of the questions concerns the role played by polarization and short-range correlation effects [9–11]: positron scattering results, in fact, are very sensitive to the detailed manner in which these effects are included in the calculations, especially at collision energies below a few eV.

When fully *ab initio* calculations are carried out [10,11], they tend to be computationally very intensive and therefore results are often limited either on the complexity of the scattering system which is being studied or on the level of completeness used in treating the long-range and short-range polarization contributions. Thus, there has been considerable interest in recent years in developing alternative treatments that employ parameter-independent models to treat polarization forces, either in the case of atomic targets or of molecular targets, for positron scattering processes [12–14].

In the present paper we are reporting the application of an alternative global modeling of positron-atom polarization forces which employs a local version of density-functional theory (DFT) for describing short-range (dynamical) correlation effects and long-range perturbation theory to treat polarization forces. We will show in the following section that such a functional form is well suited for describing positron scattering processes, especially for treating dynamic effects in the short-range region of the correlation-polarization forces. The general theory is outlined in Sec. II, while Sec. III reports our present calculations and compares them with available experiments and with other theoretical treatments. Our final conclusions are presented in Sec. IV.

II. THE THEORETICAL MODEL

When one chooses a local representation of the polarization interaction, one may qualitatively consider three different regions in the physical space of the atomic or molecular target [15]. At large distances from the target the form of the interaction could be given by a simple and familiar expression which contains the spherical, multipole polarizabilities of the target atom and holds both for electrons and positron as projectiles:

$$V_{\text{pol}}(r_p) \sim \sum_{l=1}^{\infty} \frac{\alpha_1}{2r_p^{2l+2}} \ . \tag{1}$$

It is the asymptotic limit of the multipole polarization potential when is only given by second-order perturbation-theory contributions [16]. As one moves nearer to the target, however, Eq. (1) no longer characterizes correctly the polarization effects and therefore higher-order, intermediate-range corrections need to be included, albeit still is an adiabatic, local form. It has been pointed out by various model studies [17,18] that in this region of interaction the sign of the perturbing charge becomes important and therefore model treatments introduced for electron projectiles cannot be used directly for protons as projectiles. We will further discuss this point below when describing our present approach.

Finally, as the positron projectile penetrates within the atomic or molecular charge density one further source of error becomes important as the adiabatic approximation breaks down and nonadiabatics effects play an increasingly important role. Here the adiabatic approximation usually overestimates correlation contributions, leading to a polarization potential which is too attractive, since it does not allow for the virtual positronium formation which should occur in this region. This is a different effect from the velocity-dependent corrections which should be included in the case of electron scattering, whereby the electron's kinetic energy becomes locally comparable with that of the bound electrons. This latter feature comes from the strongly attractive, short-range static exchange potential well which exists for electron scattering but is absent for the positron scattering processes. Because the static potential is now repulsive, velocity-dependent effects are less important and the positronium formation becomes the dominant nonadiabatic feature: it should occur gradually as the projectile penetrates the molecular charge cloud.

The global approach that we employ in the present calculations tries to describe as best as possible the correlated motion of each bound electron within the atomic or molecular target by giving the following ansatz for the N-electron target wave function:

$$\Phi_{\text{exact}}(x_1 \cdots x_n) = \Phi_{\text{HF}}(x_1 \cdots x_n)(1+\sigma) \ , \tag{2}$$

where x_i stands for both spatial and spin coordinates, Φ_{HF} is the "exact" Hartree-Fock (HF) wave function, and σ is a correlation correction in the short-range region. It accounts for the dynamical aspects of correlation effects, those related to the cusp conditions for each electron-electron interaction within the target charge cloud [19]. If one can further exploits the following definition for the target electronic density, $\rho(\mathbf{r})$, where the spin part has been now integrated out and $\mathbf{r}$ stands collectively for all the electronic coordinates:

$$\rho_{\text{exact}}(\mathbf{r}) \cong \rho_{\text{HF}}(\mathbf{r}) \tag{3}$$

then one can show [19] that the correlation factor for each two-electron case, $f_C(\mathbf{r}_1,\mathbf{r}_2)$, is given by

$$f_C(\mathbf{r}_1,\mathbf{r}_2) = \tfrac{1}{2}\left[1 - \frac{P^{(2)}_{\text{exact}}(\mathbf{r}_1,\mathbf{r}_2)}{P^{(2)}_{\text{HF}}(\mathbf{r}_1,\mathbf{r}_2)}\right] \ , \tag{4}$$

where the $P^{(2)}$ are now second-order density matrices without spin, derived from the wave functions of Eq. (2). This relation tells us that the correlation energy for the bound electrons can be obtained simply as a correction to the mean value of the electron-electron repulsion energy if Eq. (3) can be considered realistic, i.e., when long-range correlation effects (static correlation) play a negligible role [20].

The conclusion drawn earlier on from the above considerations [21,22] was that one could approximate the correlation energy, E_C within the target electrons, by using an expression of the following type:

$$E_C(N) \cong -\tfrac{1}{2}\int P^{(2)}_{\text{HF}}(\bar{\mathbf{r}},\bar{\mathbf{R}}) f_c(\bar{\mathbf{r}},\bar{\mathbf{R}}) \frac{d\bar{\mathbf{r}}\, d\bar{\mathbf{R}}}{2} \ , \tag{5}$$

where instead of $(\mathbf{r}_1,\mathbf{r}_2)$ we have introduced now the equivalent pair of variables: $\bar{\mathbf{R}} = \frac{1}{2}(\mathbf{r}_1+\mathbf{r}_2)$; $\bar{\mathbf{r}} = (\mathbf{r}_1-\mathbf{r}_2)$. Several suggestions by various authors [21,23] produced different choices for $f_C(\bar{\mathbf{r}},\bar{\mathbf{R}})$ and provided the correlation energy as a direct, local functional of the target electronic density. We have discussed this derivation in detail earlier on [19,24] and will not be repeating it here. Suffice it to say, however, that the evaluation of the correlation energy as a functional of the target density, and given by the specific form derived for $f_C(\bar{\mathbf{r}},\bar{\mathbf{R}})$ in Eq. (4) [19], is based on the following physical picture [24]: (i) The bound electron system is well described by a single-determinant (SD), Hartree-Fock (HF) wave function and therefore in the particular system being studied it is assumed that static correlation forces play a secondary role. (ii) The above density-functional-theory (DFT) approach only deals with short-range, dynamic correlation forces due to direct electron-electron interaction and averages over the velocity-dependent effects by a convolution over the target global charge density as given by second-order density matrices.

The next step in the derivation allows one to obtain a specific expression for the short-range correlation potential experienced by a type of pointlike incoming charge by simply performing the functional derivative of the E_C expression of before with respect to the target electronic density in the region of strong overlap between the projectile and the target density [24]. We shall call the ensuing local potential the DFT correlation-potential (DFTCP) function:

$$\begin{aligned} V_{\text{CP}}^{\text{DFT}} &= \frac{\partial}{\partial\rho} E_C[\rho(r)] \\ &= -a(F_1'\rho + F_1) - abC_F\rho^{5/3}\left[G_1'\rho + \frac{8}{3}G_1\right] - \frac{ab}{4}[G_1''\rho|\nabla\rho|^2 + G_1'(3|\nabla\rho|^2 + 2\rho\nabla^2\rho) + 4G_1\nabla^2\rho] \\ &\quad - \frac{ab}{72}[3G_1''\rho|\nabla\rho|^2 + G_1'(5|\nabla\rho|^2 + 6\rho\nabla^2\rho) + 4G_1\nabla^2\rho] \ , \end{aligned} \tag{6}$$

where the parameters a, b, c, and d were given in Ref. [23]

$$F_1[\rho(\mathbf{r})]=[1+d\rho^{-1/3}] , \tag{7a}$$

$$G_1[\rho(r)]=F_1(r)\rho^{-5/3}\exp(c\rho^{-1/3}) , \tag{7b}$$

$$C_F=\tfrac{3}{10}(3\pi^2)^{2/3} . \tag{7c}$$

The symbols with primes correspond to the first and second derivatives of F_1 and G_1 with respect to $\rho(r)$. The functional form of $V_{\rm CP}^{\rm DFT}$ for values of r larger that a given r_c is now taken to be given by the asymptotic form of Eq. (1) while the corresponding short-range expression for separate α-spin and β-spin contributions is given by

$$\begin{aligned} V_{\rm CP}^{\rm DFT}(r)=&-a(F_2'\rho+F_2)-2^{-5/3}abC_F(G_2'(\rho_\alpha^{8/3}+\rho_\beta^{8/3})\tfrac{8}{3}G_2\rho_\alpha^{5/3}) \\ &-\frac{ab}{4}[\rho\nabla^2G_2+4\nabla G_2\cdot\nabla\rho+4G_2\nabla^2\rho+G_2'(\rho\nabla^2\rho-|\nabla\rho|^2)] \\ &-\frac{ab}{36}[3\rho_\alpha\nabla^2G_2+4\nabla\rho_\alpha\cdot\nabla G_2+4G_2\nabla^2\rho_\alpha+3G_2'(\rho_\alpha\nabla^2\rho_\alpha+\rho_\beta\nabla^2\rho_\beta)+G_2'(|\nabla\rho_\alpha|^2+|\nabla\rho_\beta|^2)] , \end{aligned} \tag{8}$$

where

$$F_2=\frac{\gamma(r)}{1+d\rho^{-1/3}} , \quad G_2=F_2\rho^{-5/3}\exp(-c\rho^{-1/3}) , \quad \gamma(r)=2\left[1-\frac{\rho_\alpha^2+\rho_\beta^2}{\rho^2(r)}\right] . \tag{9}$$

The value of r_c is chosen as the crossing distance between the value of the functional derivative of the correlation energy ($E_{\rm C}$) and the value of the asymptotic form of the polarization potential in Eq. (1). This choice implies that nonadiabatic corrections from short-range correlation forces begin to act within the spatial volume in which the correlation energy of the bound electrons still has an appreciable gradient with respect to $\rho(r)$. Our DFTCP results will be compared with experiments as well as with other models such as the positron correlation polarization (PCP) potential of Jain [12] and the electron correlation polarization (ECP) [25] obtained from a free-electron-gas (FEG) derivation.

It is important to point out that the above treatment of short-range correlation effects uses a DFT approach within the target electronic density and ultimately produces a local potential which is adiabatic in its explicit form. It was, however, derived by selecting an expression for the correlation factor in Eq. (5) which contains nonadiabatic effects implicitly via the specific choice of the two-electron function that it uses [19,20]. Thus, we could say that the present DFTCP potential is equally applicable to both electron and positron scattering processes in that it solely contains the correlation effects caused by the bound electrons at a given point in space. Such a choice, however, implies that it is plausible to define a local functional form without having to distinguish between the nonadiabatic effects which electrons and positrons have as projectiles on the target wave function but by constructing only their global functional dependence on the target electronic density. Since we have derived the potential of Eq. (6) without any reference to exchange forces, which are evaluated separately in the case of electron scattering processes [24], then one can also say that the nonadiabatic effects included here come solely from the electron–other-charge short-range repulsion operator averaged over target states and can be directly used for DFT positron-electron correlation forces. It still considers as negligible, however, the differences in nonadiabatic, short-range effects between electron projectiles and positron projectiles. That this is a reasonable assumption for the present case is borne out, we believe, by the calculations discussed in the next section. The full scattering potential will, of course, include the exact static repulsion part and therefore will take into account as much as possible differences which exist between target-electron and target-positron interactions below the thresholds for either electronic excitation or positronium formation.

It is also important to note that the two regions which we mentioned before, i.e., the intermediate-range (IR) and the long-range (LR) regions, are here treated differently in the sense that the LR region is obtained directly from perturbative schemes and could be described either by the simple dipole term from second-order perturbation theory as given in Eq. (1),

$$V_{\rm pol}^{D}(r_p)_{r_p\to\infty}-\alpha_0/2r_p^4 , \tag{10}$$

or by including further terms in that expansion,

$$V_{\rm pol}^{(2)}(r_p)\underset{r_p\to\infty}{\sim}-\frac{\alpha_0}{2r_p^4}-\frac{\alpha_Q}{2r_p^6}-\frac{\alpha_O}{2r_p^8} , \tag{11}$$

where α_Q and α_O are the quadrupole and octupole static polarizabilities, respectively [19], or, furthermore, by also including the effects of the higher-order coefficients coming from third-order and fourth-order perturbation theory, i.e., the hyperpolarizability terms given by

$$\begin{aligned} V_{\rm pol}^{(3)}(r_p)&\underset{r_p\to\infty}{\sim}+\tfrac{1}{2}Br_p^{-7} , \\ V_{\rm pol}^{(4)}(r_p)&\underset{r_p\to\infty}{\sim}-\tfrac{1}{24}\gamma r_p^{-8} , \end{aligned} \tag{12}$$

where B is the dipole-dipole–quadrupole hyperpolarizability and γ is the dipole-dipole–dipole-dipole hyperpolarizability [26,27]. The implication is that higher-order perturbative terms can be disregarded and that the neces-

sary corrections of the global potential in the IR region of interaction can be modeled via the use of the r_c value that is directly obtained by the crossings between the V^{DFT} of the SR region and the perturbation theory potentials from the LR region. This very point needs further analysis and will be discussed below in great detail. It is also worth noting here that other types of model calculations employing polarized-orbital treatments for outer-shell electrons [28] have been used for positron scattering off rare gases [29]. Their calculations, although more involved than the present method, agree only qualitatively with existing experiments and therefore we decide not to further discuss them in our present work.

The choice of either Eq. (10) or Eq. (11) could of course change the values of the matching radii inside which the DFT correlation is employed and therefore could affect the final values of the computed cross sections in some noticeable manner. This point will be analyzed in the next section.

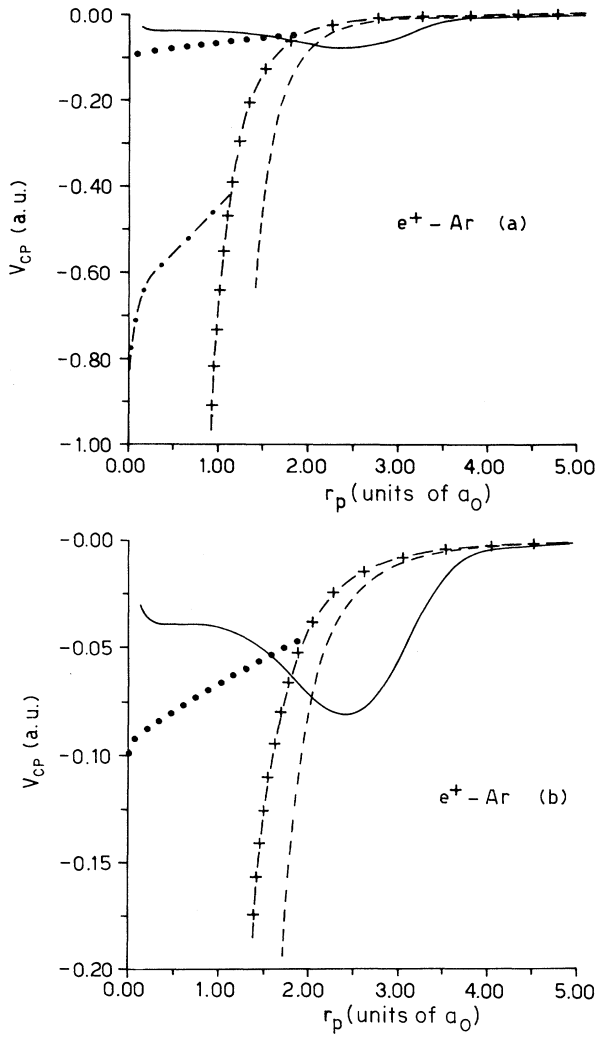

FIG. 1. Computed correlation-polarization potentials for positron-Ar interactions. -×-×-; dipole-only asymptotic potential of Eq. (10); — — —, full asymptotic potential of Eq. (11); ——, DFTCP optical potential; · · · ·, PCP optical potential; —·—·—·, ECP optical potential. (b) Enlarged part of the interaction without the ECP potential shown in the lower part of (a).

In order to compare with other theories, we have computed integral and differential cross sections for the elastic process using the free-electron–gas model of correlation potential for electron scattering processes presented earlier [24]: it will be called henceforth the ECP potential. Furthermore, we have also carried out calculations using a positron-atom potential employed earlier on by one of us [12], using the two-component DFT approach derived directly for electron-positron systems [30]. We will call them the PCP potential results.

The calculations of Fig. 1 show the relative behavior of some of these potential functions for the case of the Ar target. The upper part [Fig. 1(a)] shows a broader range of potential values, while the lower part [Fig. 1(b)] shows only a potential range of 0.2 a.u. The solid line represents the present DFTCP potential while the dashed curve reports the corresponding asymptotic potential of Eq. (11), i.e., with the inclusion of dipole, quadrupole, and octupole contributions in Eq. (1). The simple dipole results are shown by the curve with superimposed crosses. The corresponding PCP potential function is given by the dotted curve while the ECP is given only in Fig. 1(a), by the curve showing the strongest potential values and marked by data and dashes. One clearly sees both the effect of higher-order terms in the asymptotic potential and the differences between the DFTCP and the other CP potentials: they are certainly marked in the case of the ECP potential, which does not fit on the same scale as it is here a factor between 4 and 8 larger than the PCP and DFTCP potentials. These drastic differences between correlation potentials will show up accordingly in the differences exhibited by the computed cross sections discussed below and will also help us to shed more light on the most effective modeling of correlation forces in the IR regions.

III. THE COMPUTED SCATTERING OBSERVABLES

A. Integral and differential cross sections

The solution of the usual potential scattering problem requires to solve the following differential equation for each of the positron scattered radial functions ρ_l, for the lth partial wave at an energy of κ^2 in atomic units:

$$\frac{d^2}{dr_p^2}+\left\{\kappa^2-\frac{l(l+1)}{r_p^2}-2V_{\text{opt}}(r_p)\right\}\rho_l(r_p)=0\ , \qquad (13)$$

where r_p is the positron radial coordinate and $V_{\text{opt}}(r_p)$ is the present local, real optical potential for the $e^{\mp}$–rare-gas system written as a sum of the repulsive static interaction, $V_{\text{st}}(r_p)$, and the attractive correlation-polarization interaction $V_{\text{CP}}(r_p)$. The former was obtained exactly from HF target wave functions [24] while the latter was computed using the local, global models discussed in the previous section.

These radial equations were solved using Numerov's algorithm with an energy-dependent radial mesh. The

numerical details and the accuracy of the integration was more amply discussed before [24] and we will not repeat it here. Partial waves were computed using the above equation up to $l=6$, while effective-range formulas [32] were employed to calculate higher-order contributions, checking at each energy that final integral and differential cross sections converged within a 0.1% accuracy.

The different calculations, using the effective, optical potentials discussed in this work, were carried out over a broad range of energy below each positronium formation threshold for all the rare gases from He through Xe. The corresponding integral cross sections are shown in Figs. 2–6 for all the above target systems.

The solid lines show the results using the DFTCP model and the full asymptotic polarization of Eq. (11), while the dashed line reports the results using only the dipole polarizability of Eq. (10) in the LR and IR regions. The curves marked by crosses (-×-×-×) show the PCP calculations while the ECP calculations are given by the dot-dashed curves. In the case of helium, the curve denoted by pluses indicates the accurate calculations on this system carried out by Humbertson [31] a while ago. The experimental points in the various cases are given by open circles, open squares, and open triangles. They are all taken from Refs. [33,34].

In the case of He targets we clearly see that the DFTCP calculations agree remarkably well with experiments and with the earlier calculations by Humbertson (Fig. 2): in this case the simpler, dipole-only asymptotic potential provides better agreement with the very-low-energy data around the Ramsauer-Townsend (RT) type of minimum. The ECP potential is also in very good agreement with the previous data, while the PCP potential is in strong disagreement and exhibits the wrong energy dependence.

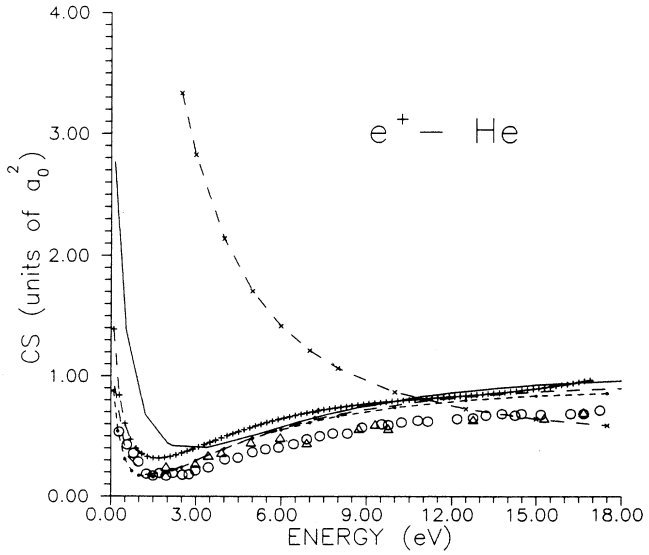

FIG. 2. Computed and measured integral elastic cross sections for positron scattering from He atoms. The experiments are 000, from Ref. [33]; △△△, from Ref. [34]. The calculations are ——, DFTCP with the full potential of Eq. (11); — — — DFTCP with dipole-only asymptotic potential; dashes with superimposed bars from Ref. [31]; -×-×-×, PCP with dipole-only asymptotic potential; —·—·—· ECP with dipole-only asymptotic potential.

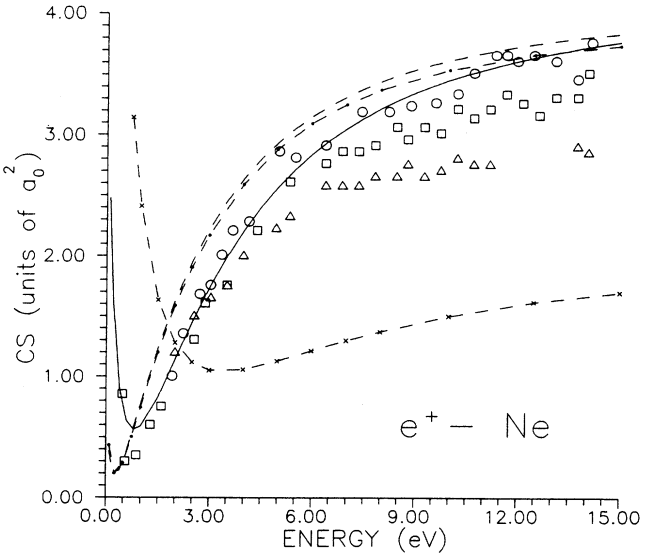

FIG. 3. Same data as in Fig. 2 but for the neon atom. The meaning of symbols is the same, with the additional experiments: □□□, from Ref. [39].

The results for a more complex system, the Ne target, are also in good agreement with experiments, as one can see from the comparison between measurements and present calculations shown in Fig. 3. One also sees from the data reported in the figure that the use of the more extended asymptotic polarization of Eq. (11) (solid-line calculations) provides the best overall agreement, while the simpler dipole-only term (dashed line) appears to be more accurate mostly in the region around the marked cross-section minimum: in that region the ECP calculations (—·—·—·) are also very close to our results and follow them up to the highest energies, while the PCP calcu-

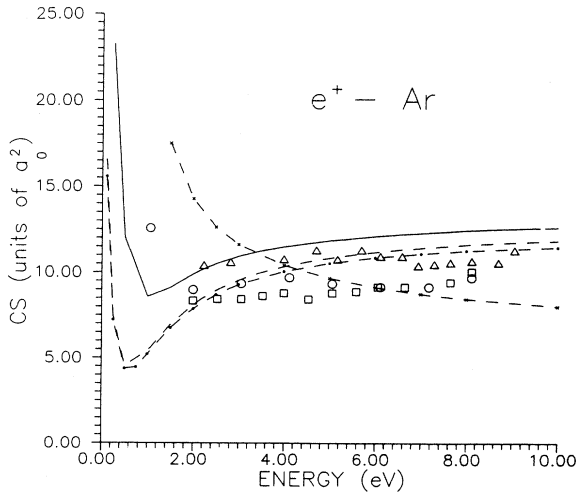

FIG. 4. Same data as in Figs. 2 and 3, but this time for the Ar atom. The meaning of the symbols is the same as before.

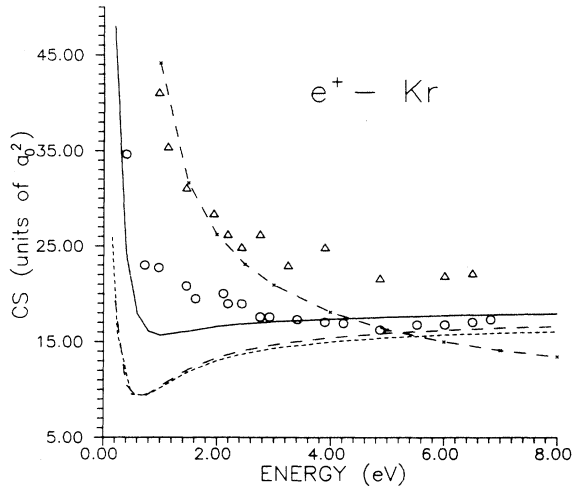

FIG. 5. Same as in the previous figures but for the case of Kr atoms as the target. The meaning of the symbols is the same as before.

lations have both the wrong energy dependence and the wrong absolute values of the cross sections with respect to experiments.

The same general trend is observed in the results for Ar atoms (Fig. 4). The experimental data are here scattered over a broader range of values, but our calculations with the full asymptotic potential form and the DFTCP optical potential (solid line) agree with them very well. The ECP and DFTCP with only dipole polarizability are once more very close to each other and close to the experiments, while the PCP optical potential fails rather markedly in reproducing the experiments.

The computational results for Kr and Xe, carried out at the nonrelativistic level, are shown in Figs. 5 and 6, respectively. The corresponding experimental results are again very different from each other and show less evidence for a low-energy minimum as one goes from Kr to Xe. Our calculations indeed agree with such a trend and do so better when using the full polarization of Eq. (11) (solid line) than with the dipole-only term (dashed curve) with the DFTCP optical potential. The ECP calculations are once more in good accord with the dipole-only-plus-DFTCP calculations, thus indicating that the optical potentials plotted in Fig. 1 only show differences as the collision energy increases, while behaving essentially in the same way in the low-energy regimes. The PCP calculations, on the other hand, produce the largest cross-section values and appear to follow only qualitatively the energy dependence of the experimental data.

To give a feeling of the induced differences in the long-range part of the present DFTCP potentials, we report in Table I the polarizability values employed in our calculations [35], together with the coefficients of the third-order perturbation theory corrections [27], which we will discuss below.

As is well known, the angular distributions of scattered positrons, even at the elastic level below the positronium formation thresholds, provide a very stringent test for the theoretical models employed in their calculations. Thus, we have carried out calculations for such quantities using the optical potential which performed the best in the previous comparison between measured and computed integral cross sections, i.e., the DFTCP potential model.

The results for Ne target are shown in Fig. 7 at a collision energy of 13.6 eV: Fig. 7(a) presents results on a logarithmic scale while Fig. 7(b) shows them on a linear scale. The experimental points are given by filled circles in both cases and come from Ref. [33]. The calculations which use the DFTCP discussed before are given by two different curves in each set of plots: the solid line results refer to using an asymptotic polarization form as given by Eq. (11), while the dashed line reports the calculations with dipole-only asymptotic potential. The agreement between calculated and measured quantities is remarkably good for both models, although the use of a more ex-

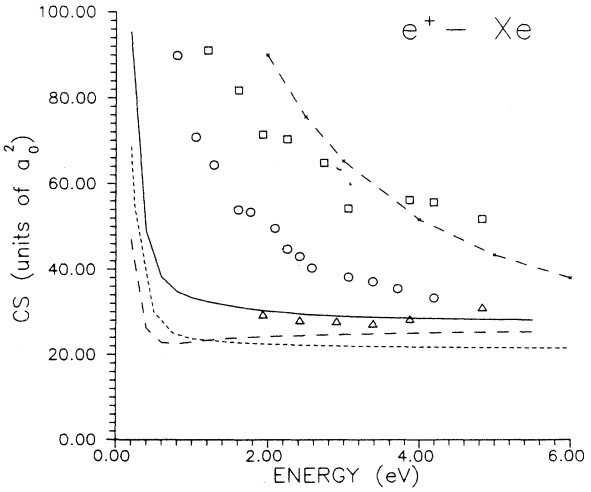

FIG. 6. Same as in previous figures but for the case of Xe atoms as the target. The meaning of the symbols is the same as before.

TABLE I. (a) Values of the dipole polarizabilities, α_D, of the quadrupole polarizabilities, α_Q and of the octupole polarizabilities, α_O, employed in the present work. All values in a.u. (from Ref. [35]). (b) Values of B and γ hyperpolarizabilities (from Ref. [27]) employed in the present work. All values in a.u. Numbers in square brackets indicate powers of 10.

	α_D	α_Q	α_O
He	1.38	2.44	10.60
Ne	2.66	6.42	30.40
Ar	11.10	52.40	490
Kr	16.70	92.7	793
Xe	27.30	170	2016

	B	γ
He	−7.347	4.190[1]
Ne	−1.775[1]	1.046[2]
Ar	−1.643[2]	1.083[3]
Kr	−3.432[2]	2.255[3]
Xe	−8.117[2]	4.877[3]

tended long-range polarization potential appears to fare slightly better. The same result was found before for the integral cross sections of Fig. 3.

The calculated and measured differential cross sections (DCS) for Ar atoms are shown in Fig. 8 for three different collision energies: at 2.18 eV [Fig. 8(a)], at 6.67 eV [Fig. 8(b)], and at 8.71 eV [Fig. 8(c)]. The filled circles report the experimental points of Refs. [33,36], while the calculated curves have the same meaning as before, when showing computed angular distributions for Ne targets.

The agreement between the solid curves and the experimental data are again rather encouraging at all energies since the calculations clearly reproduce the general drop of angular distributions as the scattering angle gets larger.

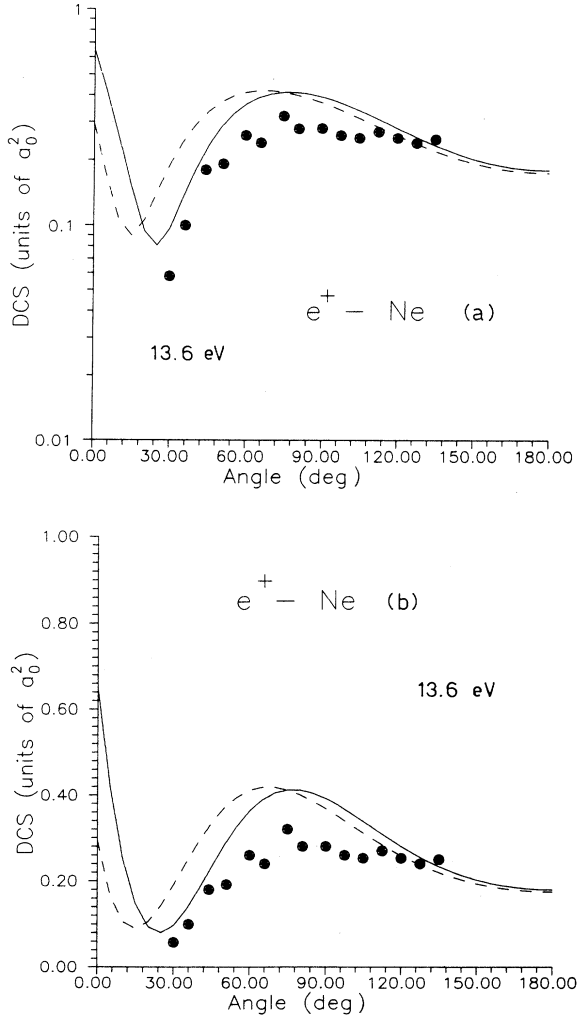

FIG. 7. Computed and measured differential cross sections (DCS) as a function of the scattering angle at a fixed energy of 13.6 eV (a) logarithmic scale; (b) linear scale, for neon atom targets. The filled circles are the experimental results from Ref. [33]. The calculations are as follows: ——, DFTCP plus the full asymptotic polarization of Eq. (11); — — —, DFTCP plus the dipole-only asymptotic polarization.

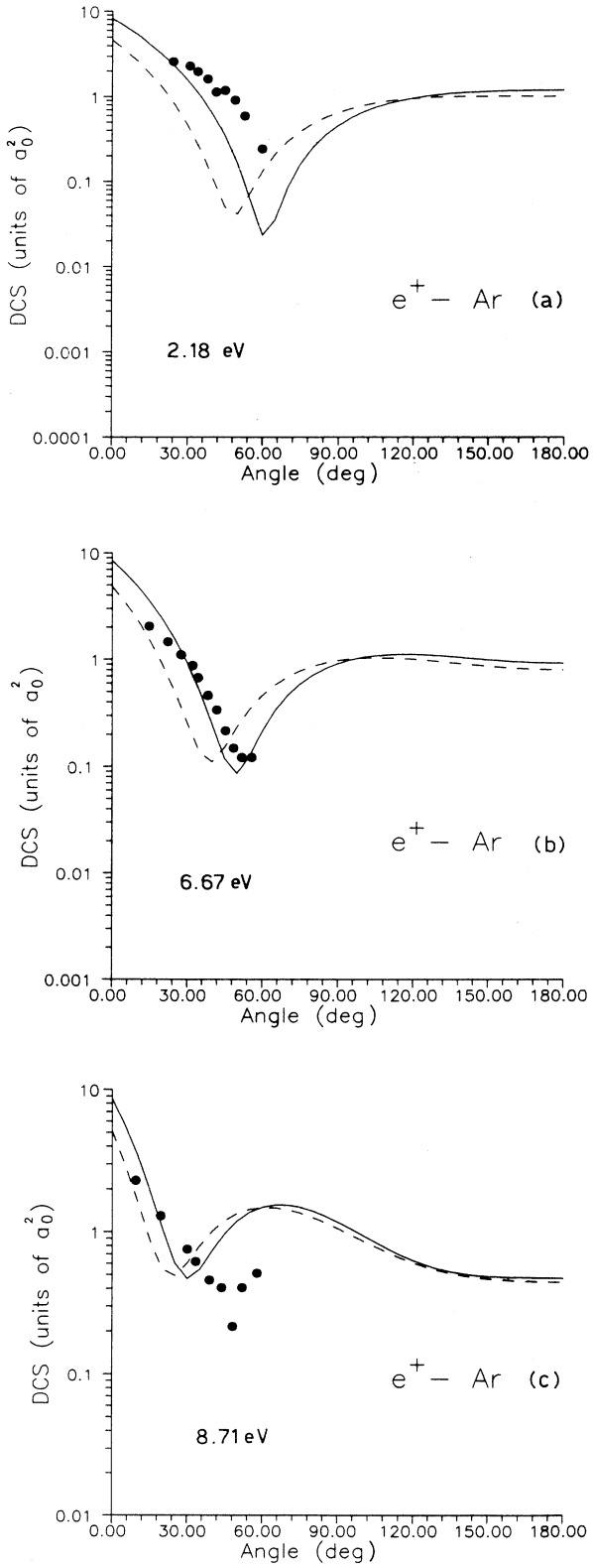

FIG. 8. Computed and measured differential cross sections (DCS) for argon targets. The experiments are the filled circles and came from Ref. [36]. (a) data and calculations at 2.18 eV; (b) at 6.67 eV; (c) at 8.71 eV. The meaning of the computed curves is the same as that for Fig. 7.

One should keep in mind that such calculations are really very easy to perform within the present model and therefore indicate the attractiveness of using our DFT approach for modeling positron scattering optical potentials, since nearly quantitative agreement with experiments is attained with a rather modest computational effort.

B. The effects of perturbation-theory series truncation

As mentioned before the present DFTCP model approach employs a specific, nonadiabatic prescription to treat short-range (SR) correlation forces and the coefficients of second-, third-, and fourth-order perturbation series expansion to describe long-range (LR) forces. The next feature of this global model is related to the way it treats the intermediate-range (IR) part of the interaction. This is that special region of configuration space in which adiabatic, higher-order effects are expected to play a role, as well as the differences in nonadiabatic effects between electrons and positrons as projectiles.

As discussed earlier, Eqs. (10) and (11) are independent of the charge of the projectile and specifically describe LR adiabatic effects. On the other hand, Eq. (12) includes third-order and fourth-order effects and the sign of its coefficients depends on the charge of the projectile. In the case of a positron, the coefficients of that equation (see Table I) are both attractive and therefore their net effect on the global potential is to move the r_c values to the outer region, thereby making the DFTCP potential stronger in the IR range of relative distances.

Figure 9 presents, in fact, the behavior of the V^{DFT} potential, for all the rare-gas targets, in the IR regions around the crossing values, r_c. The results for He atoms are shown in Fig. 9(a), while the results with increasing Z, from Ne to Xe, are shown in the figure from 9(b) to 9(e). The continuous line presents the calculations with the DFTCP model; the line with stars, the dipole polarization potential of Eq. (10); the line with crosses, the full polarization potential of Eq. (11); while the line with pluses presents the additional contributions of the higher-order coefficients of Eq. (12) and Table I.

The following behavior can be extracted from examining the results shown in the figure.

(i) As expected from physical intuition, the crossing values, r_c, increase substantially from He to Xe and go from about $2.0a_0$ up to about $5.0a_0$. On the other hand, the ECP model and the PCP model show a less marked variation with the "size" of the atomic charge densities.

(ii) The complete interaction with contributions up to third-order perturbation-theory (PT) terms decreases more slowly with r_p and therefore always exhibits the largest r_c values for each system. Hence, the DFTCP short-range contributions are extended more into the IR region when such a potential is employed.

(iii) As Z increases, the larger r_c values imply that the crossing region falls into energy ranges which are smaller and therefore our description of the IR effects moves outwards and produces weaker potentials. This result seems to indicate that for the light atoms the choice of Eq. (10), (11), or (12) to describe the V_{pol} part of the full interaction produces more drastic differences in the description of the IR region of the potential than it does for systems such as Kr or Xe.

(iv) The heavier atomic targets show that, because of the larger values of r_c, the DFT correlation follows very closely the curve with crosses in the outer region, while the lighter atoms have their potentials markedly changed after the crossings.

In sum, the comparison discussed above indicates that the full correlation-polarization potentials describe the IR region rather differently when one changes the V_{pol} contributions, depending on whether one considers light atomic targets or atomic targets with several electrons.

The same type of differences are provided by the integral cross-section calculations. To make the comparison clearer, we show in Fig. 10 only the computed cross sections obtained from the $V_{\mathrm{CP}}^{\mathrm{DFT}}$ potential and with different forms of V_{pol} as discussed before. The range of energy shown is the same as that of Figs. 2–6, where the other model potentials and the experimental data were also presented. The sequence of the different atomic targets goes from the helium target, in Fig. 10(a), to the xenon target, in Fig. 10(e).

The results given by the solid line present, as before, the cross sections computed with the V_{pol} of Eq. (11), while those given by the dashed line refer to the user of the dipole term only in the asymptotic region. The curve marked by pluses shows the calculations carried out with the higher-order terms of Eq. (12) added to the V_{pol} of Eq. (11). One can draw the following conclusions from an examination of the results of the figure.

(i) For the lighter atomic targets, He and Ne, the calculations which employ only the dipole potential of Eq. (10) agree the best with the experiments of Figs. (2) and (3) and describe well the cross-section minima in the low-energy region. The higher-order PT contributions make the IR region potential stronger and yield cross sections which are too large.

(ii) For the heavier atoms, Ar, Kr, and Xe, the higher terms in the PT expansion correctly eliminate any low-energy minimum in the computed cross sections and make them more in agreement with experiments, as one can see from a perusal of Figs. 4–6 with the experimental results.

(iii) At the higher collision energies, and below the positronium formation threshold, the various long-range choices of V_{pol} affect the computed cross sections only very little and the latter are essentially entirely coincident for the case of the lighter atoms.

In conclusion, the test of different PT series truncation on computed cross sections and on the global shape of our proposed DFTCP model suggests that, for light atoms, the IR region interaction should be described by the weakest possible potential model while for heavier atomic targets the higher terms of the PT series are needed in order to yield a stronger interaction potential for positron projectiles.

IV. DISCUSSION AND CONCLUSIONS

We presented in the previous sections a comparison between different parameter-free model potentials for treat-

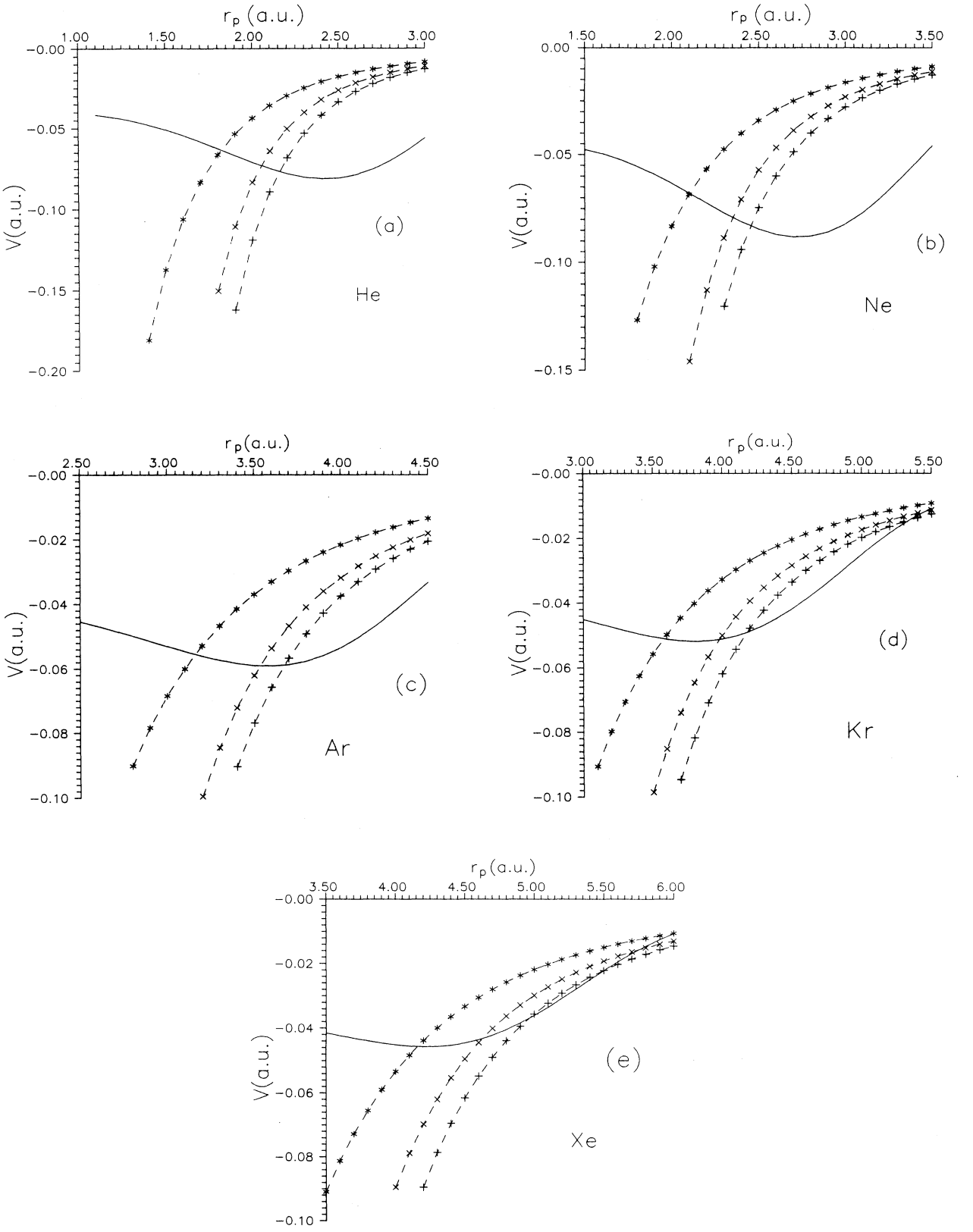

FIG. 9. Computed correlation-polarization potentials using the V_{CP}^{DFT} model in the short-range region and different V_{pol} in the LR region: -*-*-*, potential of Eq. (10); -×-×-×, potential from Eq. (11); -+-+-+, potential of Eqs. (11) plus (12). (a)–(e) refer to helium through xenon targets, respectively.

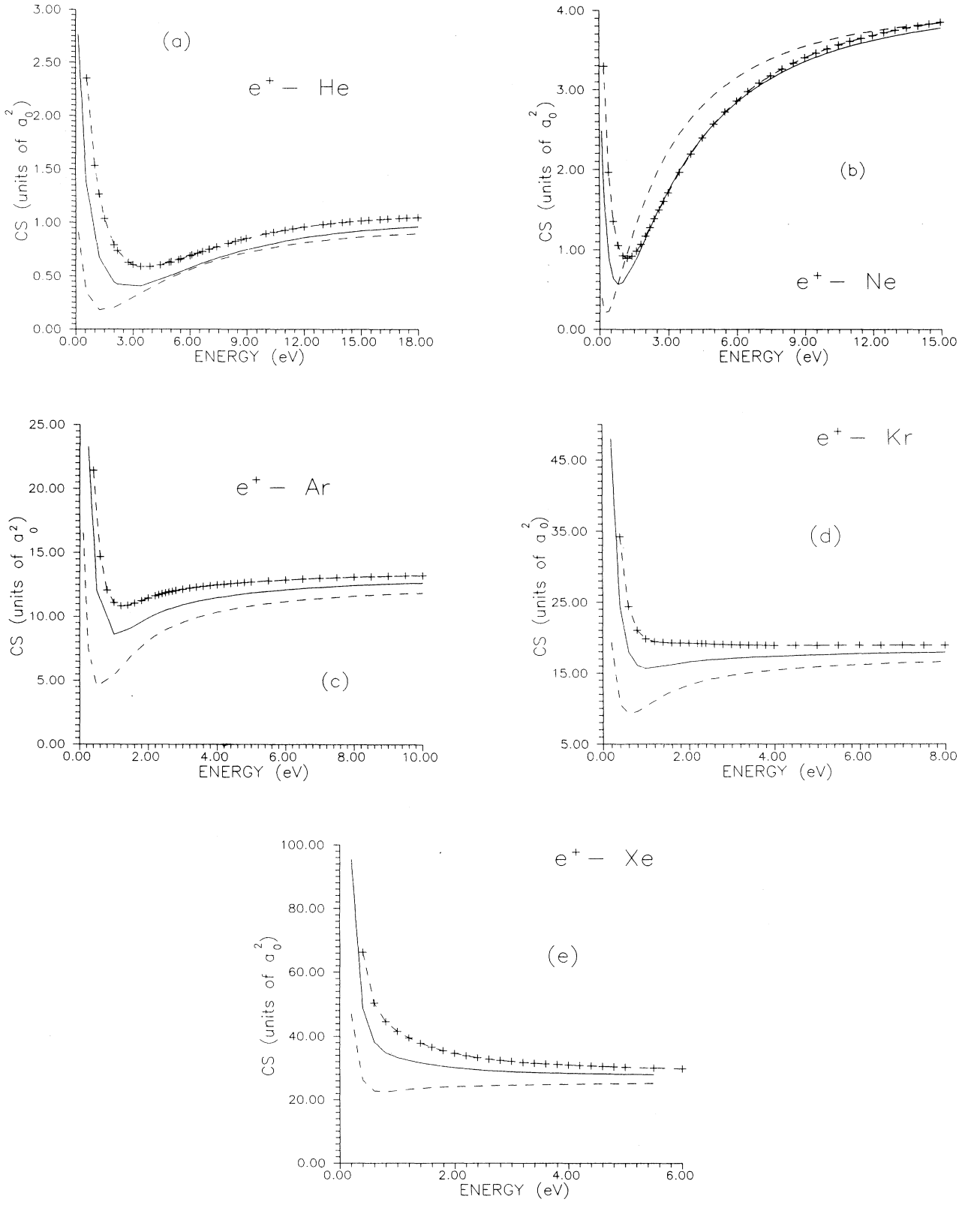

FIG. 10. Computed integral elastic cross sections using the DFTCP potential forms of Fig. 9. The various curves, as a function of energy, refer to the different models: ——, V_{pol} from Eq. (11); — — —, V_{pol} from Eq. (10); -+-+-+, V_{pol} from Eqs. (11) plus (12). (a)–(e) refer to helium through xenon as target atoms.

ing positron scattering processes from rare gases at low collision energies. The general aim of such potentials was to generate, using physically realistic simplifications, local, energy-independent forms of optical potentials for scattering processes below the positronium formation thresholds. Thus, we presented an approach based on density-functional theory, which we labeled the DFTCP optical potential, whereby the repulsive static interaction was obtained exactly from HF target wave functions while the short-range nonadiabatic polarization effects were included in a global form as functional derivatives with respect to the target electronic densities of N-particle correlation energy, E_C. The basic assumption of that approach was, as mentioned earlier, that the dynamic correlation effects could be given in local form and therefore the nonlocal differences between electrons and positrons as interacting projectiles with the N bound electrons could be considered as small. Since the original derivation [19–24] for electron scattering processes clearly separated exchange effects from direct correlation effects, then the DFTCP potential could be used for positron scattering under the assumption that the nonlocal, virtual excitation processes in the two cases differ rather little from each other, in spite of their different physical origins [18].

Furthermore, we have employed a recently proposed short-range correlation potential which had been obtained for positron-electron interactions where the bound electrons were treated as a homogeneous-electron-gas model [12,30]. We have called such a potential the PCP potential model and found it to be only qualitatively in agreement with experiments, with its behavior at higher energies being closer to them than the one in the low-energy regimes. The third model which we have employed in our calculations is the one suggested earlier for treating electron scattering short-range correlation effects [25], and which used a free-electron-gas model of the target system. We call it the ECP optical potential in the present work and used the dipole-only asymptotic polarization as its long-range part. The results of our calculations indicate that the ECP model agrees rather closely with our DFTCP potential in the low-energy regimes but departs from it as the collision energy increases towards the positronium formation threshold: for more complex target atoms its computed cross sections are invariably smaller than the experimental data and smaller than those from the DFTCP potential calculations. We have also carried out a detailed analysis of truncating at various levels the PT series coming from the LR region of interaction, thereby modifying within our model the description of the interaction in the IR region. Our analysis shows that differences in the computed cross sections only appear at very low collision energies, while from intermediate energies and up to the positronium threshold the various contributions affect cross sections only rather weakly.

Both angular distributions and integral cross-section calculations indicate here that the DFTCP approach produces quantities which agree remarkably well with the available experiments and is well suited for describing short-range correlation effects in positron scattering below threshold. Such effects are here essentially given by a DFT model designed for electron scattering processes. In other words, although one is aware of the fact that the physics of positron interaction with the target electronic cloud is different from that of an electron projectile, especially in the short-range region where nonadiabatic, energy-dependent virtual excitations come from different processes in the two cases [37,38], one can nevertheless effectively employ a local model approach where an energy-independent, real optical potential is produced from DFT. From the computational evidence of the present comparison, one therefore could conclude that in the low-energy scattering regimes the types of effective potentials which are generated for electron scattering correlation effects via density-functional models also can be applied for positron scattering calculations in spite of the differences in the physical processes which give rise to those short-range nonlocal effects. On the other hand, light and heavy targets show marked changes in their computed cross sections at very low collision energies when the LR treatment via a PT series is truncated at different terms, the latter also being different from those for electrons for positrons. Both angular-distribution data and integral cross-section data indicate here the realistic quality of the DFTCP and ECP models and the rather poor performance of the PCP model potential. How such an analysis could be extended to molecular systems is the subject of our current work on diatomic and polyatomic targets and will be presented elsewhere.

ACKNOWLEDGMENTS

The financial support of the Italian National Research Council (CNR) is gratefully acknowledged. One of us (J.A.R.-R.) thanks the EEC for financial support at the University of Rome under a Science Collaborative Project. A NATO collaboration project between the University of Rome and Florida A&M University is also acknowledged for its financial support of short visits by the two principal investigators. Finally F.A.G. is grateful to the Institute for Theoretical Atomic and Molecular Physics (ITAMP) at the Harvard-Smithsonian Center for Astrophysics for a financial support while this work was completed.

*Address for correspondence: Dipartimento di Chimica, Città Universitaria, 00185 Rome, Italy.

[1] For example, E. A. G. Armour, Phys. Rep. **169**, 1 (1988).

[2] K. F. Canter and A. P. Mills, Jr., Can. J. Phys. **60**, 551 (1982).

[3] K. Floeder, P. Honer, W. Raith, A. Schwab, G. Sinapius, and G. Spicher, Phys. Rev. Lett. **23**, 2363 (1988).

[4] S. J. Smith, G. M. A. Hyder, W. E. Kauppila, C. K.

Kwan, and T. S. Stein, Phys. Rev. Lett. **57**, 2252 (1986).
[5] L. Dou, W. E. Kauppila, C. K. Kwan, and T. S. Stein, Phys. Rev. Lett. **68**, 2913 (1992).
[6] L. Dou, W. E. Kauppila, C. K. Kwan, D. Przybyla, S. J. Smith, and T. S. Stein, Phys. Rev. A **46**, R5327 (1992).
[7] M. Charlton, T. C. Griffith, G. R. Heyland, and G. L. Wright, J. Phys. B **16**, 333 (1983).
[8] O. Sueoka and S. Mori, J. Phys. Soc. Jpn. **53**, 2491 (1984).
[9] B. K. Elza, T. L. Gibson, M. A. Morrison, and B. C. Saha, J. Phys. B **22**, 113 (1989).
[10] E. A. G. Armour, D. J. Baker, and M. Plummer, J. Phys. B **23**, 3057 (1990).
[11] J. Tennyson and L. Morgan, J. Phys. B **20**, L641 (1987).
[12] A. Jain, Phys. Rev. A **41**, 2437 (1991).
[13] T. L. Gibson, J. Phys. B **23**, 767 (1990).
[14] A. Jain and F. A. Gianturco, J. Phys. B **24**, 2387 (1991).
[15] M. A. Morrison and B. C. Saha, Phys. Rev. A **34**, 2786 (1986).
[16] For example, see L. Castillejo, I. C. Percival, and M. J. Seaton, Proc. R. Soc. London, Ser. A **254**, 259 (1960).
[17] M. Morrison, T. L. Gibson, and D. Austin, J. Phys. B **17**, 2725 (1984).
[18] M. Morrison, in *Positron (Electron) Gas Scattering*, edited by W. E. Kauppila, T. S. Stein, and J. M. Wadhera (World Scientific, Singapore, 1986), p. 100.
[19] F. A. Gianturco and J. A. Rodriguez-Ruiz, J. Mol. Structure (Theochem) **260**, 99 (1992).
[20] R. Colle and O. Salvetti, J. Chem. Phys. **93**, 534 (1990).
[21] R. Colle and O. Salvetti, Theor. Chim. Acta **37**, 329 (1975).
[22] R. Colle and O. Salvetti, Theor. Chim. Acta **53**, 55 (1979).
[23] C. Lee, W. Yang, and R. G. Parr, Phys. Rev. B **37**, 785 (1988).
[24] F. A. Gianturco and J. A. Rodriguez-Ruiz, Phys. Rev. A **47**, 1075 (1993).
[25] J. K. O'Connell and N. F. Lane, Phys. Rev. A **27**, 1893 (1983).
[26] A. D. Buckingham, Adv. Chem. Phys. **12**, 107 (1967).
[27] G. Maroulis and A. J. Thakkar, J. Phys. B **21**, 3819 (1988).
[28] R. P. Mc Eachran, A. D. Stauffer, and L. E. M. Campbell, J. Phys. B **13**, 1281 (1980).
[29] R. P. Mc Eachran, D. L. Morgan, A. G. Ryman, and A. D. Stauffer, J. Phys. B **10**, 663 (1977).
[30] E. Boronski and R. M. Nieminen, Phys. Rev. B **34**, 3820 (1986).
[31] J. W. Humbertson, J. Phys. B **6**, L305 (1973).
[32] T. F. O'Malley, L. Spruch, and L. Rosenberg, J. Mol. Phys. **2**, 491 (1961).
[33] S. J. Smith, G. M. A. Hyder, W. E. Kauppila, C. K. Kwan, and T. S. Stein, Phys. Rev. Lett. **64**, 1227 (1990).
[34] T. S. Stein and W. E. Kauppila, Adv. At. Mol. Phys. **18**, 53 (1982).
[35] A. A. Ratzig and B. M. Smirnov, *Reference Data on Atoms, Molecules and Ions* (Springer, Berlin, 1985).
[36] P. J. Coleman and J. D. McNutt, Phys. Rev. Lett. **42**, 1130 (1979).
[37] F. A. Gianturco, Europhys. Lett. **12**, 689 (1990).
[38] T. L. Gibson, J. Phys. B **23**, 767 (1990).
[39] M. Charlton, Rep. Prog. Phys. **48**, 737 (1985).